Gravitational Wave Astronomy: A New Window to the Cosmos

Dr. Omar López-Cruz
Instituto Nacional de Astrofísica, Óptica y Electrónica
Astrofísica
omarlx@inaoep.mx

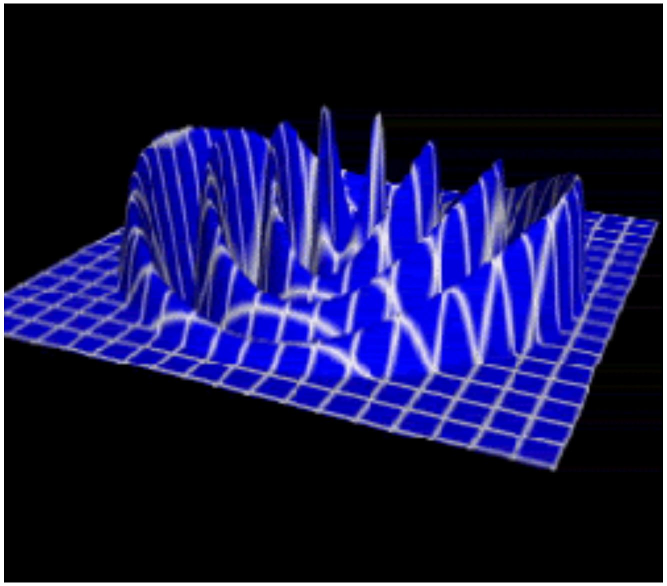

http://focus.aps.org/story/v8/st3

www.jointsolutions.co.uk/ docs/ pages/leftnav.htm

According to Einstein's theory of gravity, an accelerating mass causes the fabric of space-time to ripple like a pond disturbed by a rock. These ripples are Gravity Waves.

This picture represents Gravity Waves produced by a pair of rotating neutron stars.

This picture represents ripples in a pond disturbed by a rock.

Electromagnetic Waves

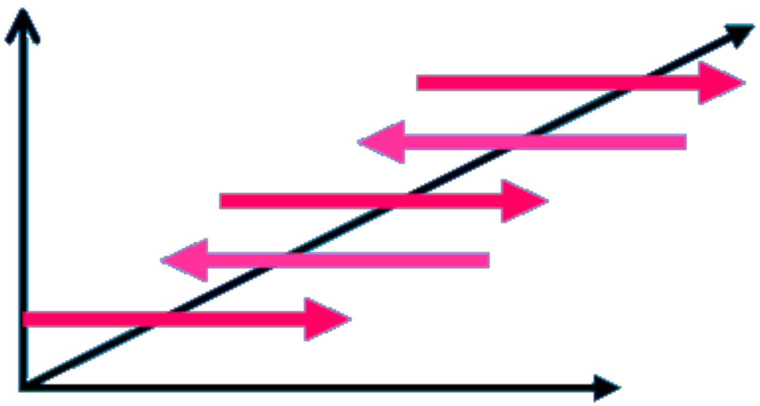

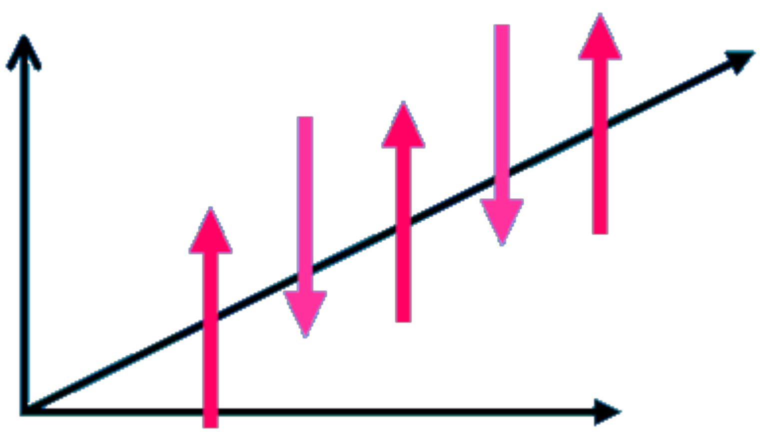

Electromagnetic Waves oscillate perpendicular to their motion.

They oscillate in the X and Y directions and the wave moves in the Z direction.

Gravity Waves

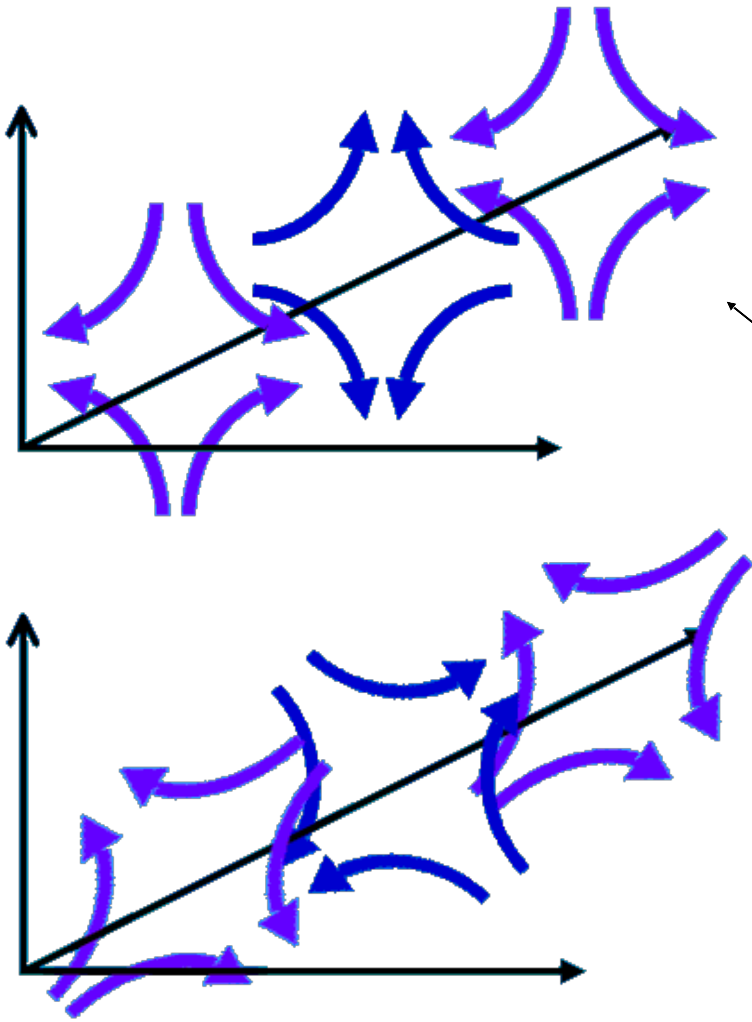

Gravity waves have 2 polarizations like Electromagnetic Waves. The only difference is that Gravity Wave polarization lies in a horizontal-vertical “+” shape and 45 degrees to that in a “x” shape.

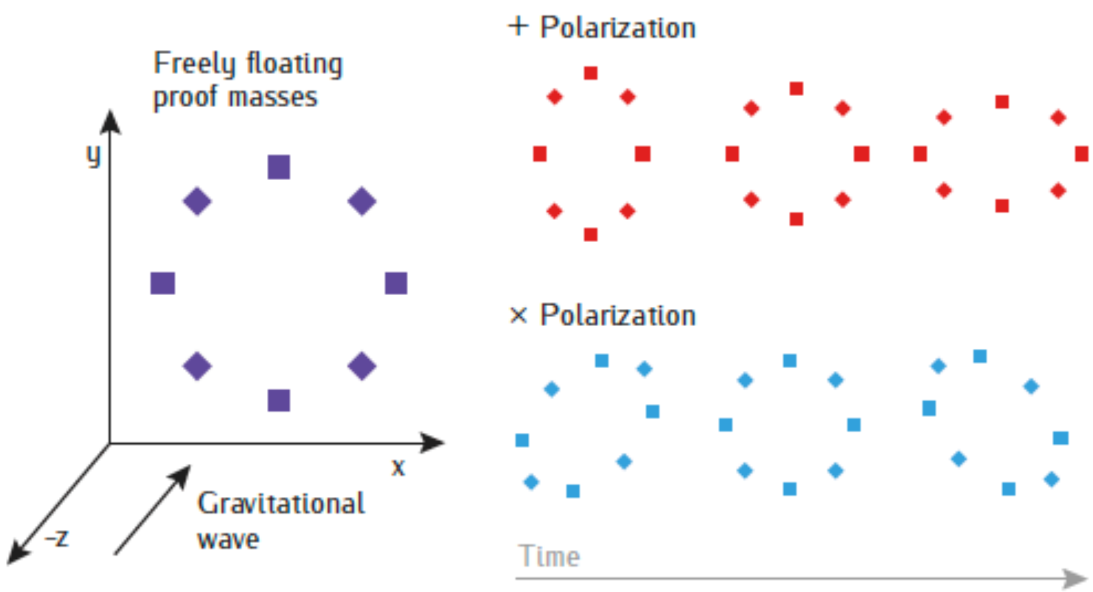

Figure 1.8: A ring of proof masses freely floating in the xy-plane and a gravitational wave that propagates along the z-direction. While a +-polarized wave will change the proper distance in x and y directions, the influence of a ×-polarized wave is rotated by 45° so that distances along the x- and y-axis remain unaffected.

Why are they important?

Gravity Waves would give us a new way to observe the universe. Like a new sense, they would bring a new dimension to astronomy.

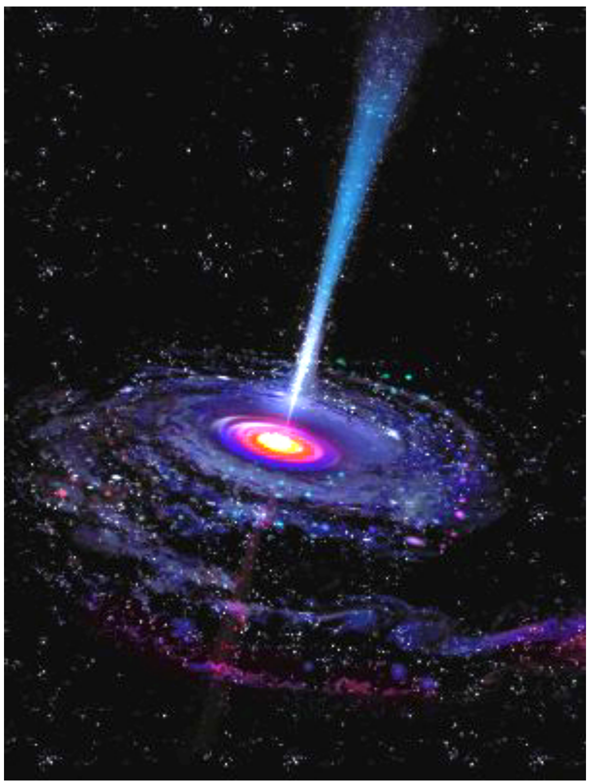

They would:

Verify general relativity's prediction that gravity waves exist.

Test that they travel at the speed of light.

Test that the graviton has zero rest mass.

Study black holes, and a binary black hole system.

Allow us to study astronomical entities that we either know little about, or have yet to discover.

Gravitational Radiation

Gravitational Radiation, for example, occurs in a binary system with two massive objects circling one another. The large accelerations due to their gravitational attraction would release gravitational radiation. The noticeable affect of the expelled radiation is the loss of mechanical energy of the system, the two circling objects would draw closer to one another.

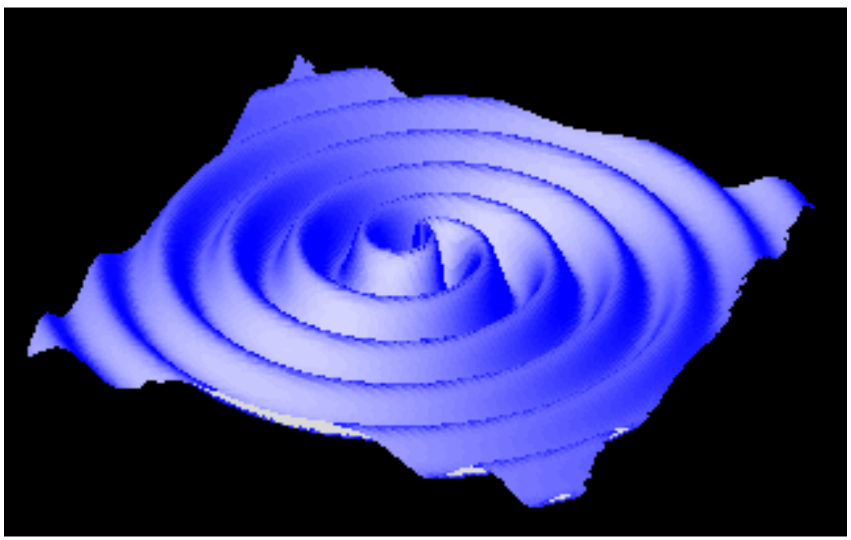

Laser Interferometer

A laser is split into two beams and aimed down either arm.

The beams reflect off a mirror at the end, return to the middle, bounce back to the end, and back to the middle for a total of 50 times. This makes the distance the light travels longer, and increases the sensitivity of the detector.

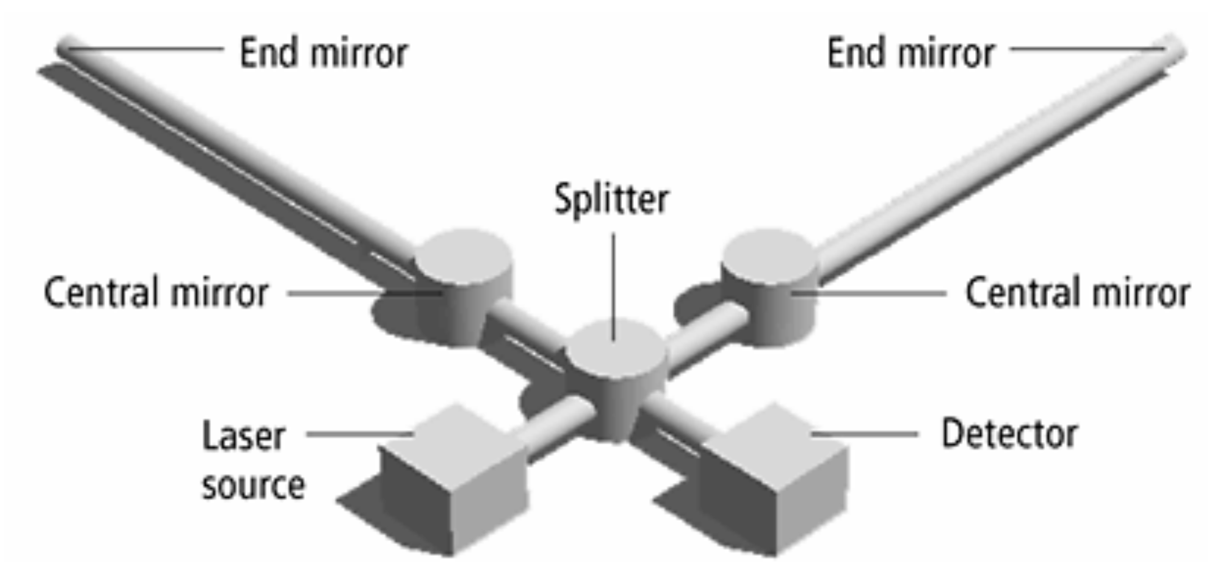

Gravitational Wave Detection

- Suspended Interferometers
  - » Suspended mirrors in "free-fall"
  - » Michelson IFO is "natural" GW detector
  - » Broad-band response (~50 Hz to few kHz)
  - » Waveform information (e.g., chirp reconstruction)

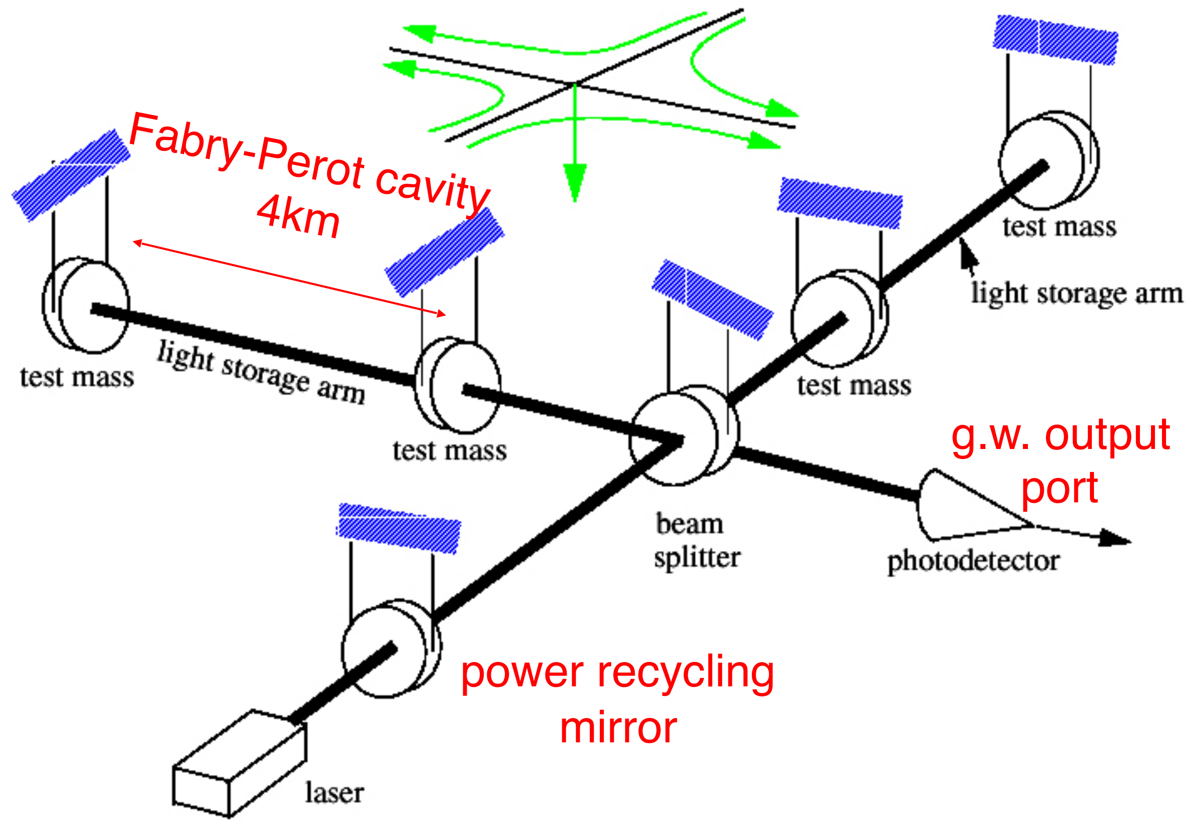

LIGO design length sensitivity: 10^{-18}m

LIGO mirrors

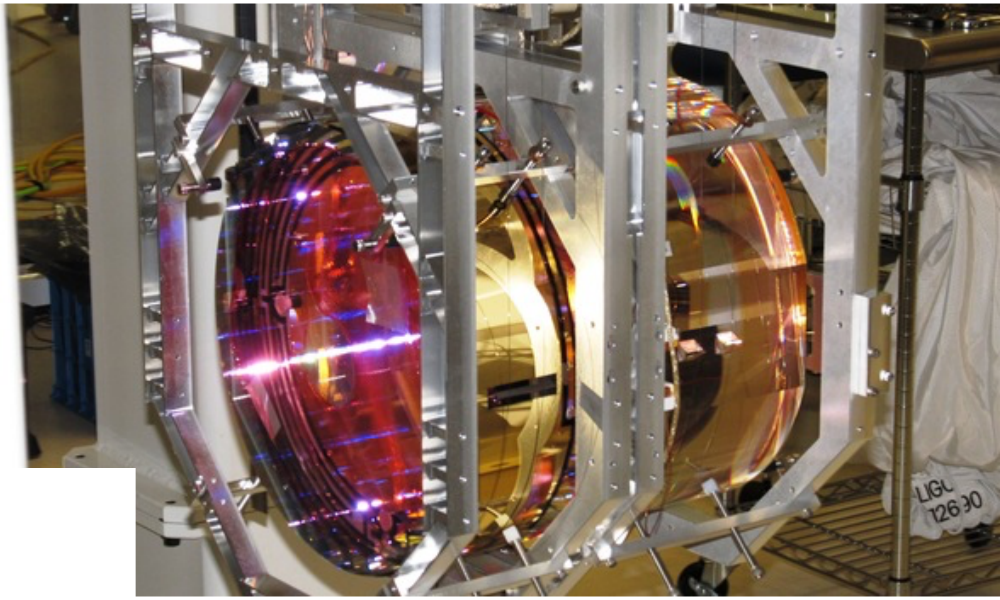

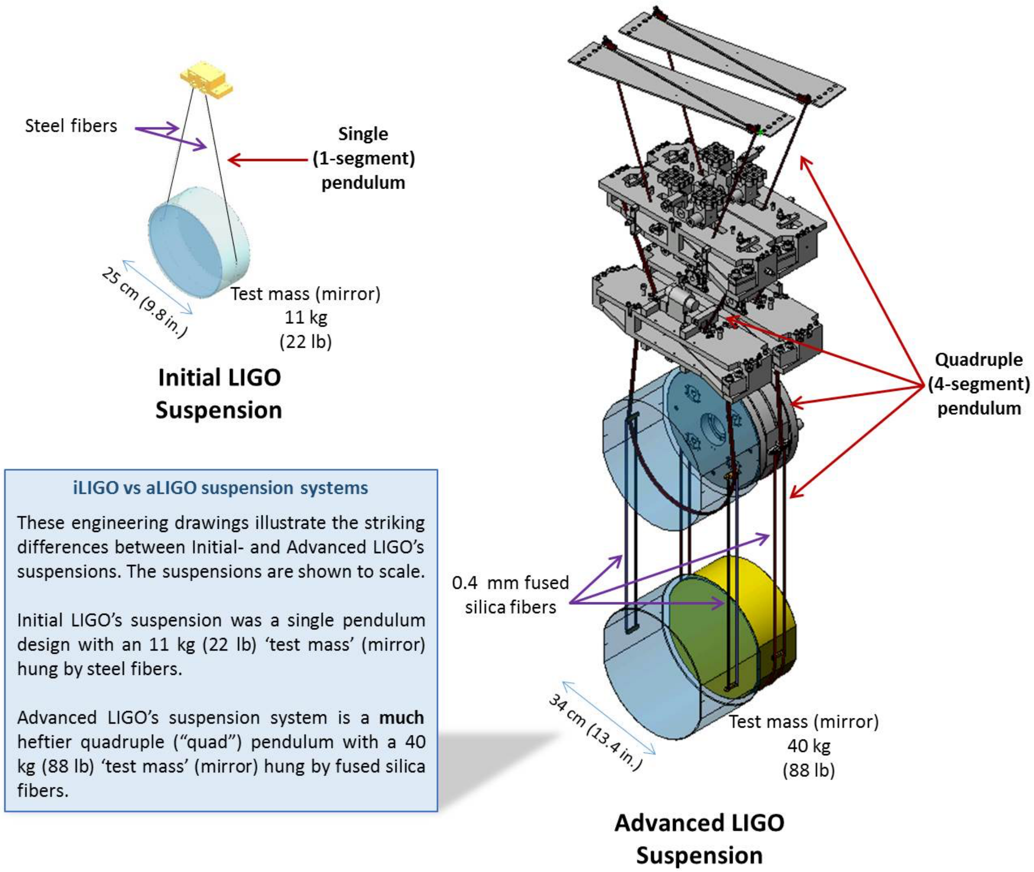

LIGO Sensing the Effect of a Gravitational Wave

Gravitational wave changes arm lengths and amount of light in signal

Change in arm length is 10^{-18} meters, or about 2/10,000,000,000,000,000 inches

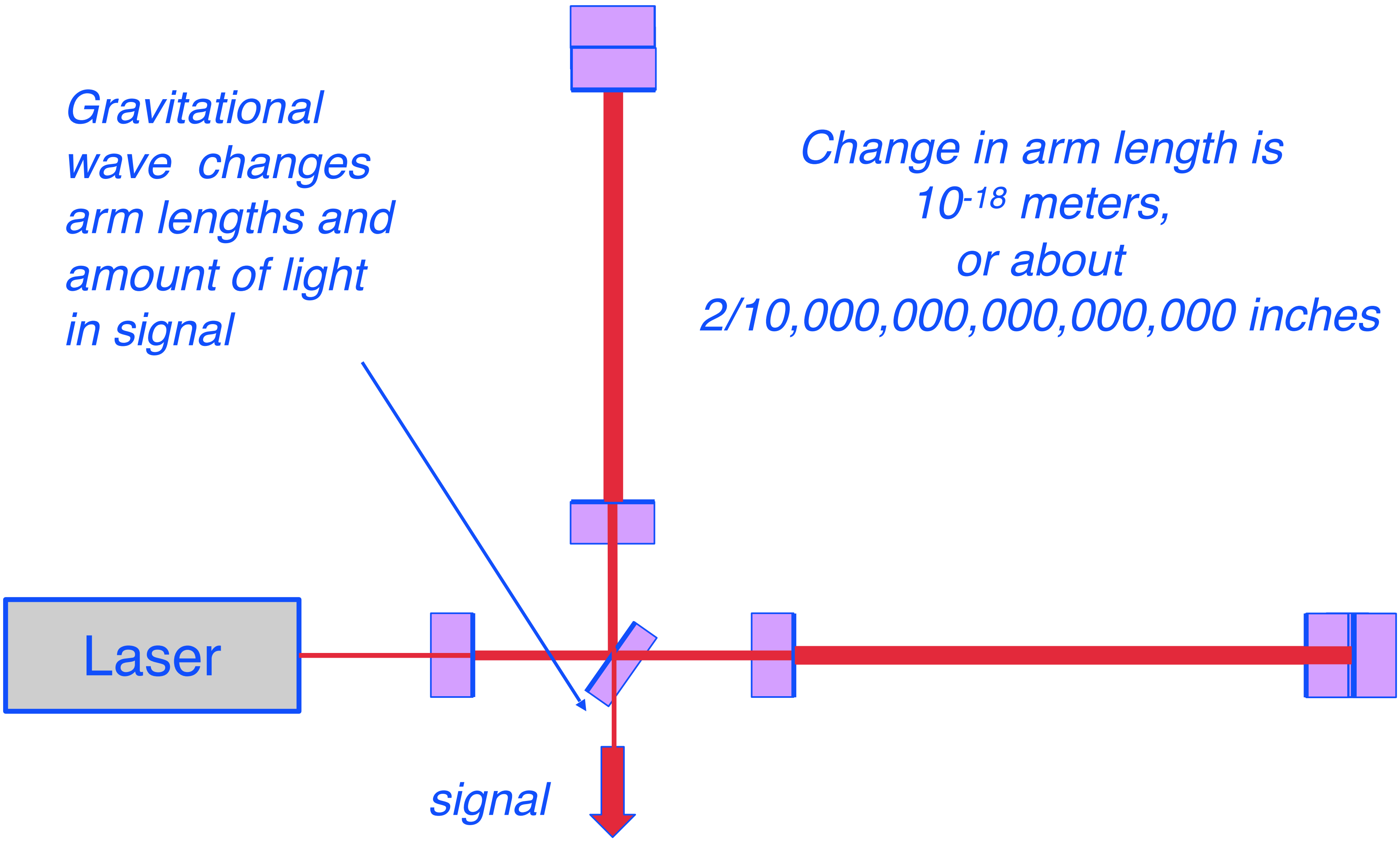

LIGO sites

LIGO (Washington)
(4km and 2km)

LIGO (Louisiana)
(4km)

Funded by the National Science Foundation; operated by Caltech and MIT; the research focus for more than 670 LIGO Scientific Collaboration members worldwide.

The LIGO Observatories

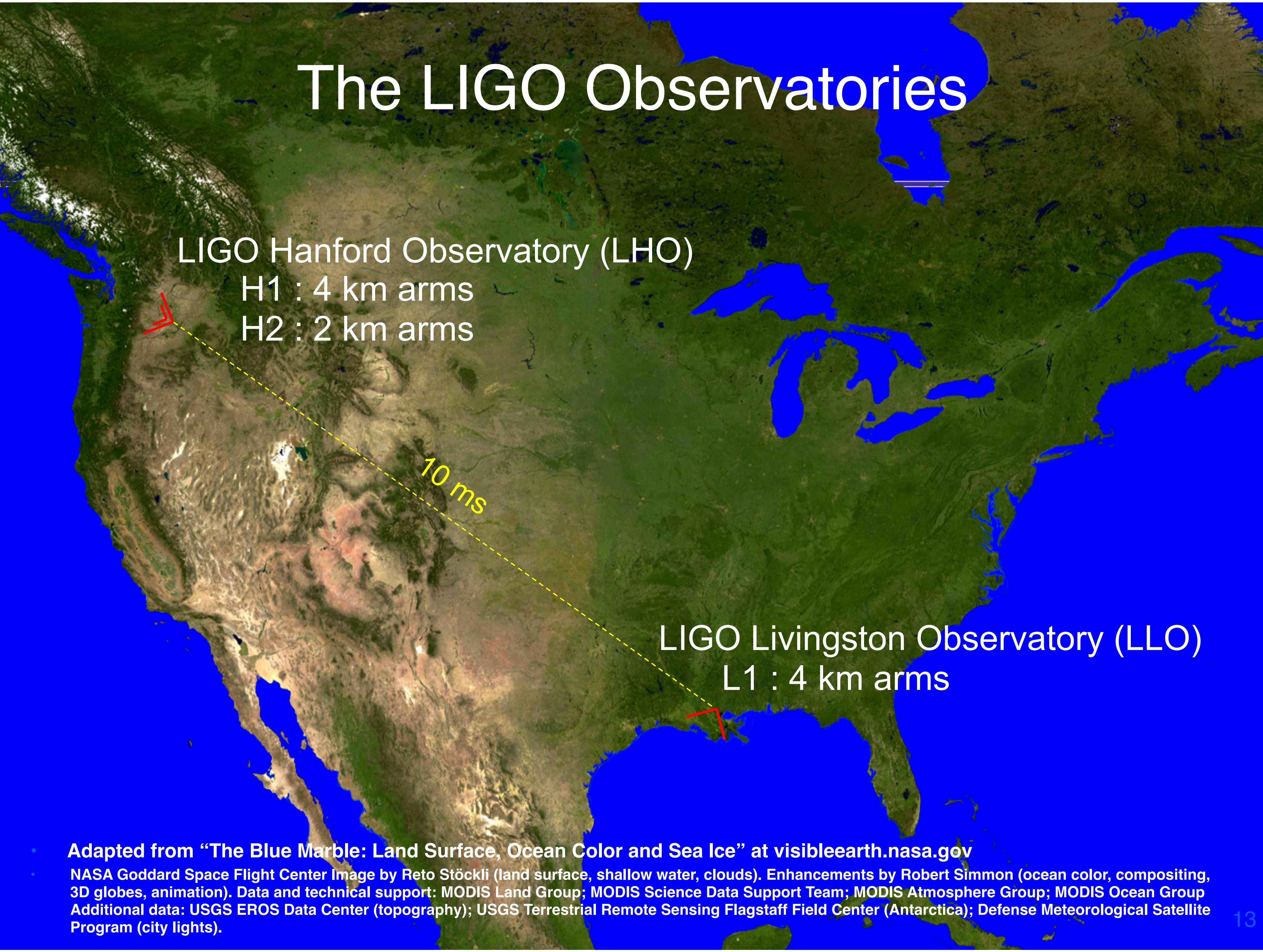

- **Adapted from "The Blue Marble: Land Surface, Ocean Color and Sea Ice" at visibleearth.nasa.gov**
- **NASA Goddard Space Flight Center Image by Reto Stöckli (land surface, shallow water, clouds). Enhancements by Robert Simmon (ocean color, compositing, 3D globes, animation). Data and technical support: MODIS Land Group; MODIS Science Data Support Team; MODIS Atmosphere Group; MODIS Ocean Group Additional data: USGS EROS Data Center (topography); USGS Terrestrial Remote Sensing Flagstaff Field Center (Antarctica); Defense Meteorological Satellite Program (city lights).**

The First Detection

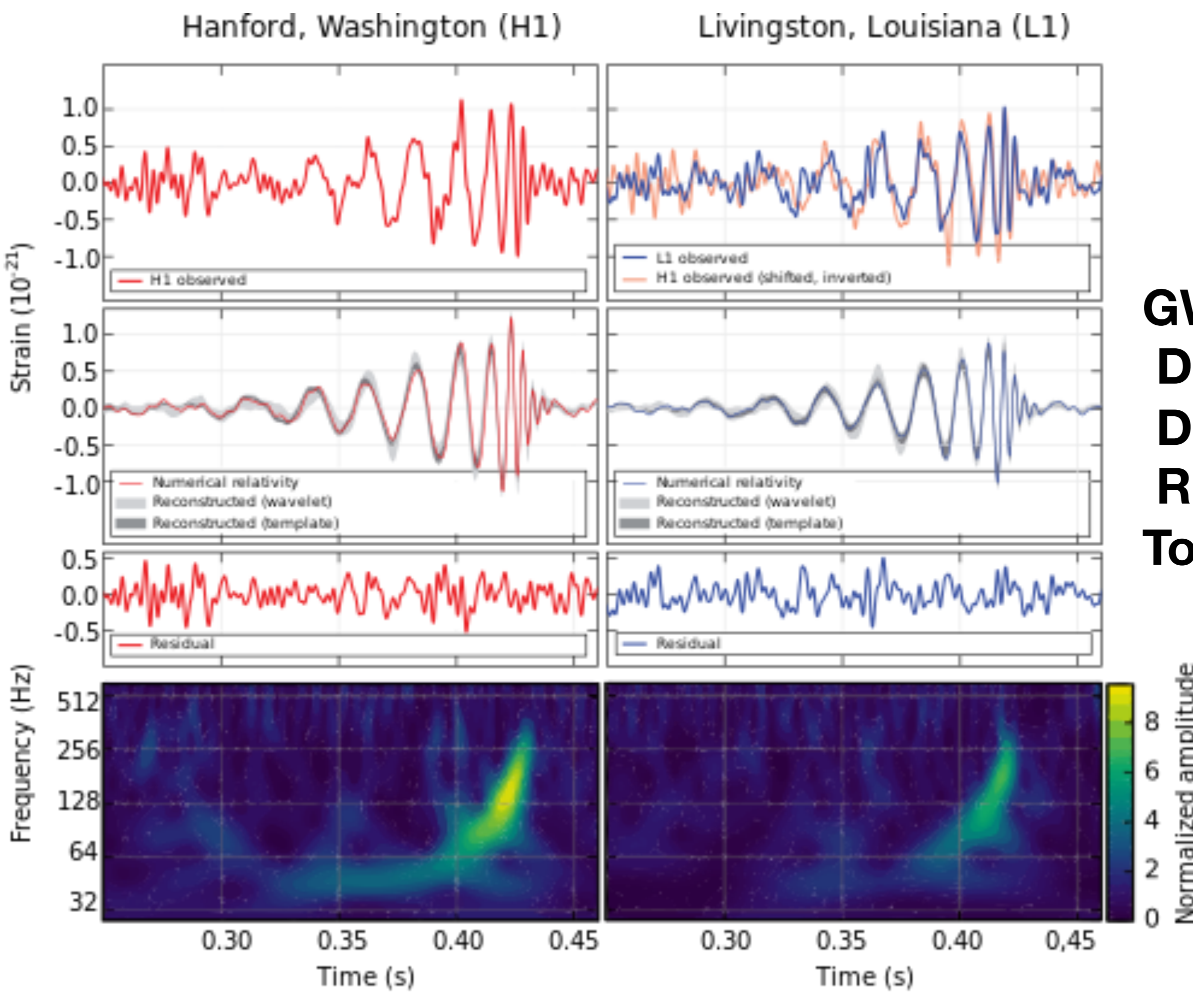

GW150914
Duration 0.2 sec
Distance 440(+160-180) Mph
Redshift 0.093 (+0.030-0.036)
Total energy imput 3 (+/-0.5) Msun

Previous Events

- GW150914 Advanced LIGO
- GW 151226 Advanced LIGO
- GW 170104 Advanced LIGO
- GW 170814 Advanced LIGO + VIRGO

- All of these event ware due to BH mergers

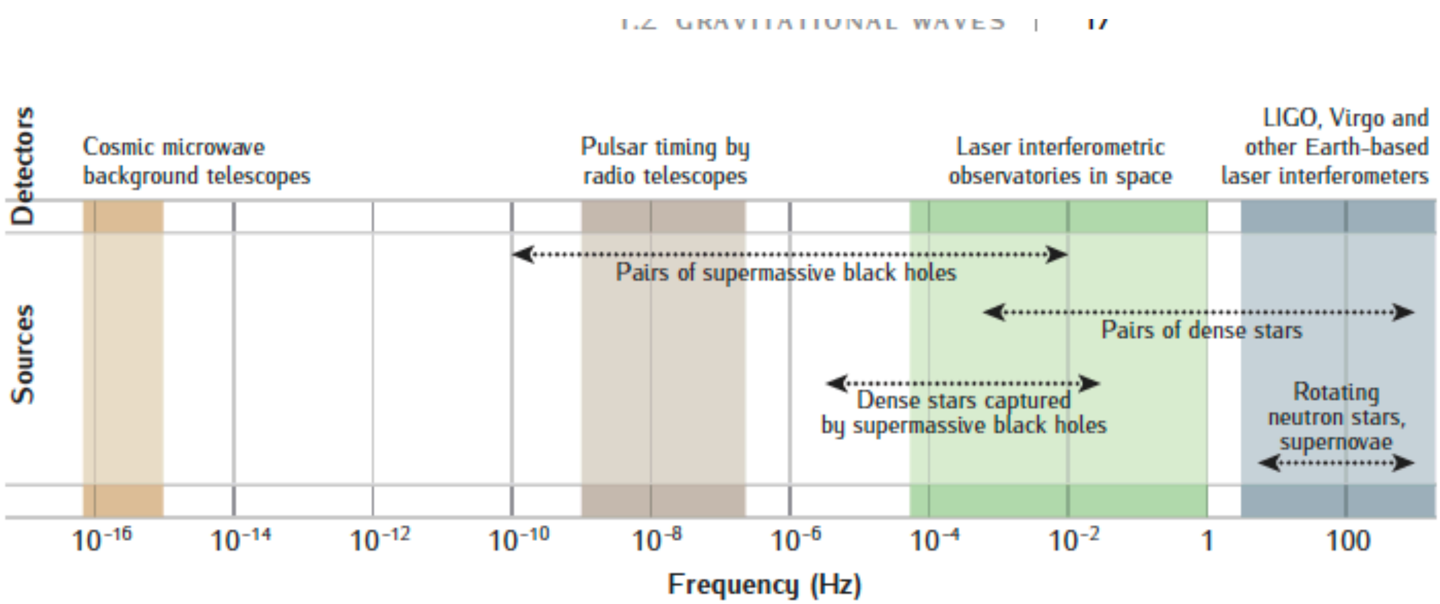

GW170817

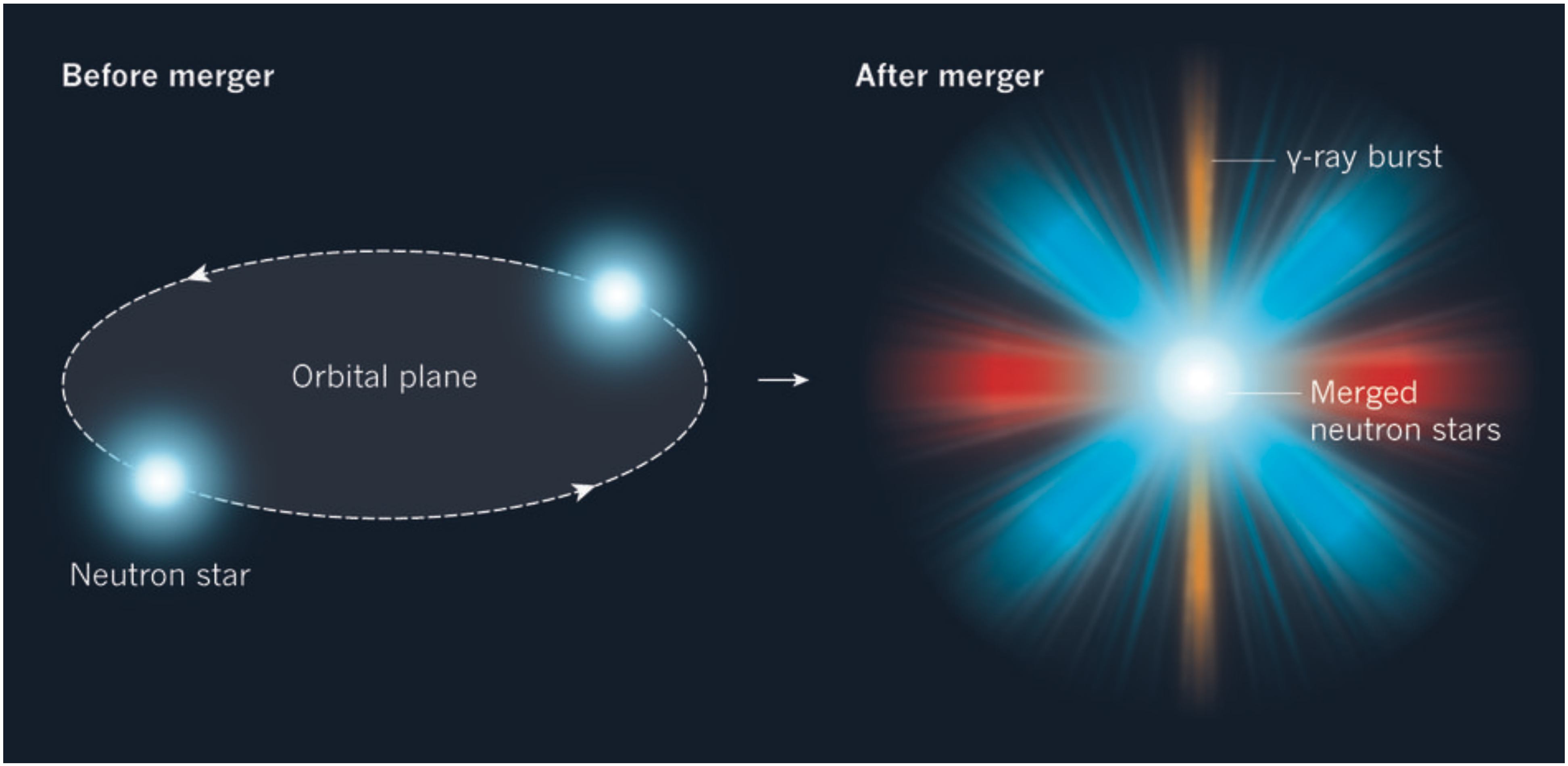

Before merger
Orbital plane
Neutron star
After merger
γ-ray burst
Merged
neutron stars

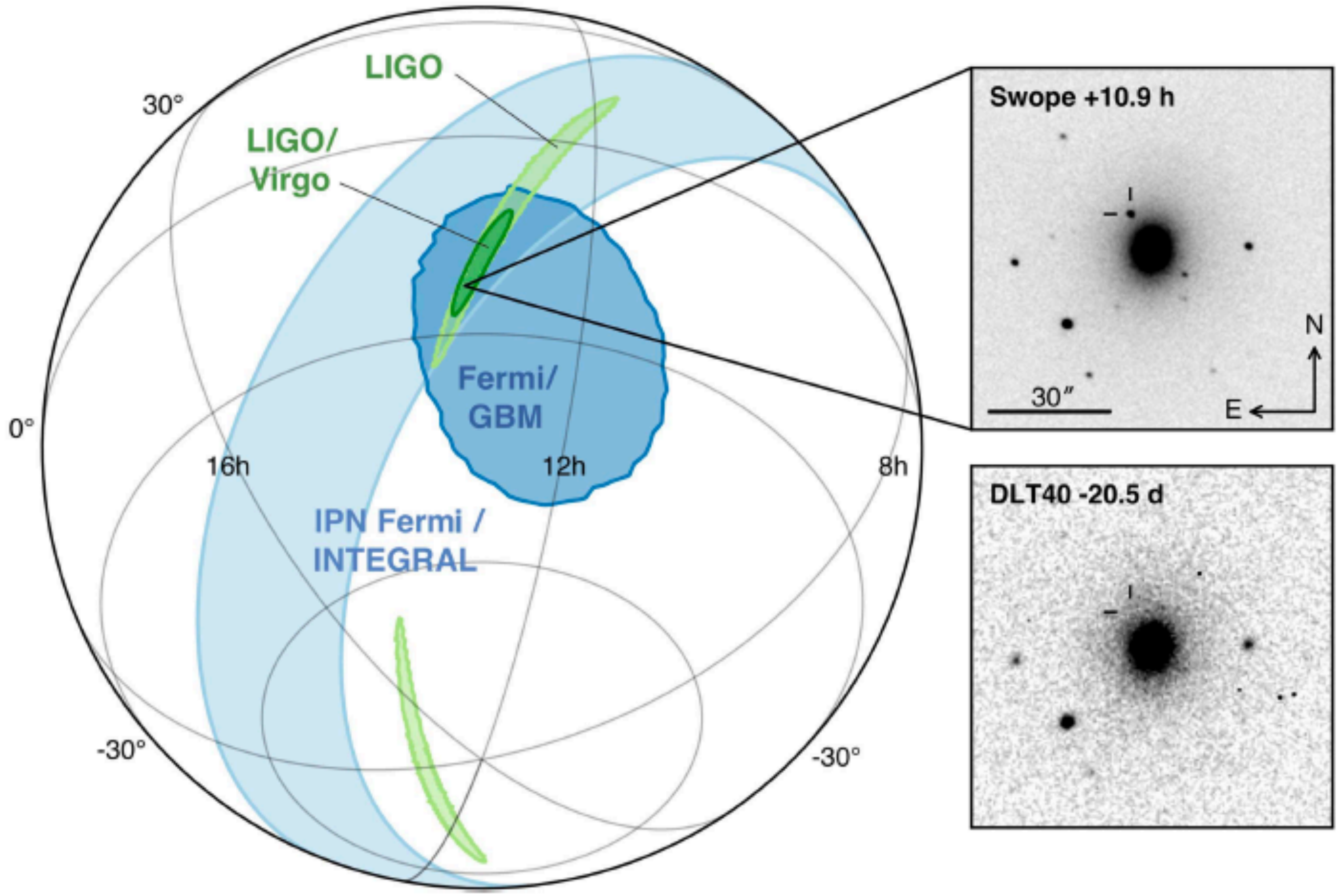

Figure 1. Localization of the gravitational-wave, gamma-ray, and optical signals. The left panel shows an orthographic projection of the 90% credible regions from LIGO (190 deg^2; light green), the initial LIGO-Virgo localization (31 deg^2; dark green), IPN triangulation from the time delay between *Fermi* and *INTEGRAL* (light blue), and *Fermi*-GBM (dark blue). The inset shows the location of the apparent host galaxy NGC 4993 in the Swope optical discovery image at 10.9 hr after the merger (top right) and the DLT40 pre-discovery image from 20.5 days prior to merger (bottom right). The reticle marks the position of the transient in both images.

Localizations of the gravitational wave, the γ-ray burst and the kilonova on the sky

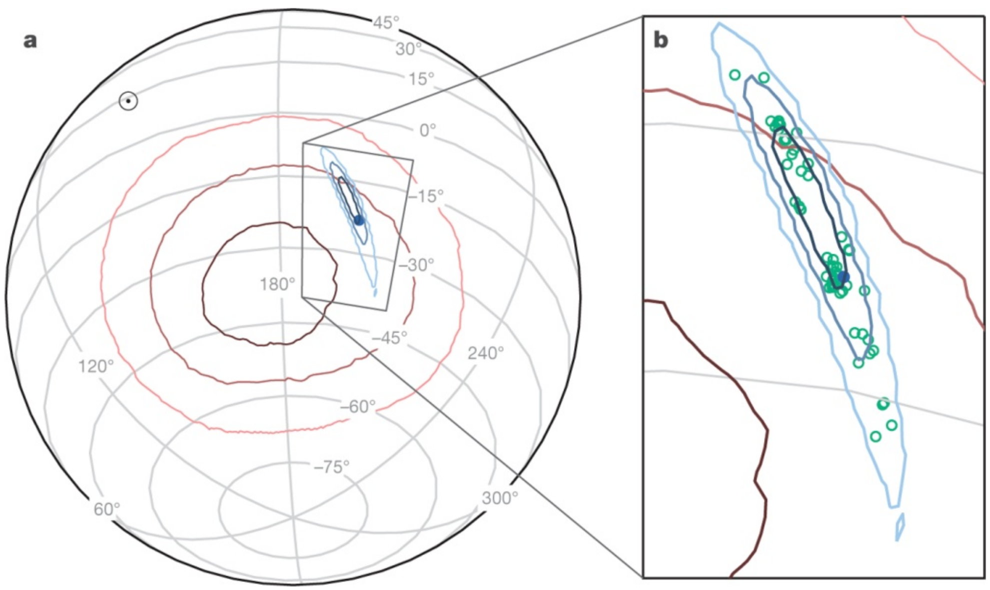

I Arcavi *et al. Nature* 1–3 (2017) doi:10.1038/nature24291

nature

The TOROS Collaboration

1m class telescope

Gemini Observatory, 8m Telecope

Gran Telescopio Canarias, 10m Telescope

LCO discovery image of the kilonova AT 2017gfo in the galaxy NGC 4993

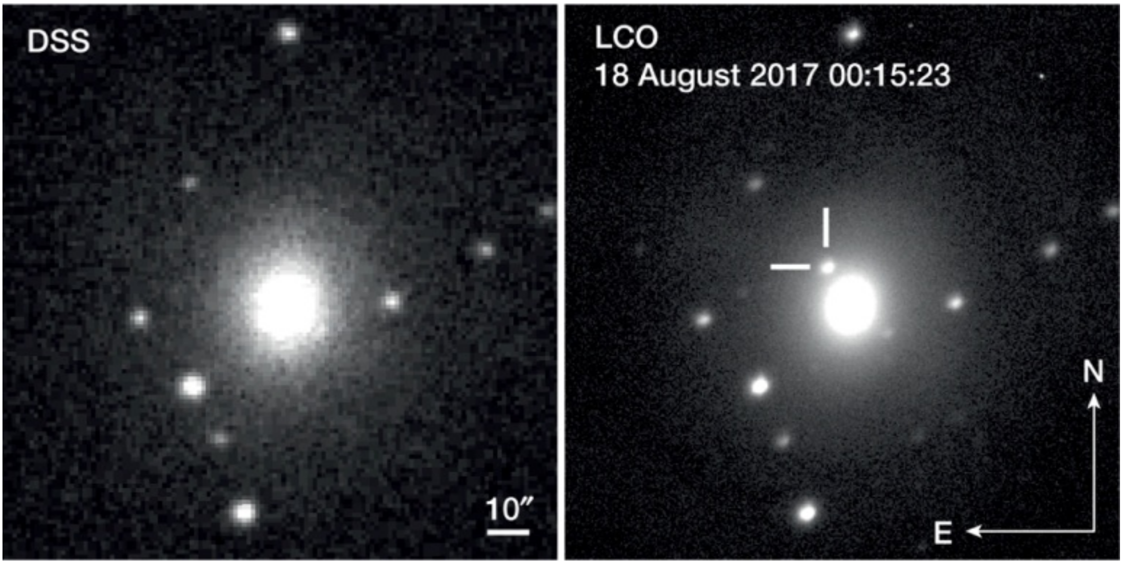

RA 13:09:48.1
DEC -23:22:53

I Arca

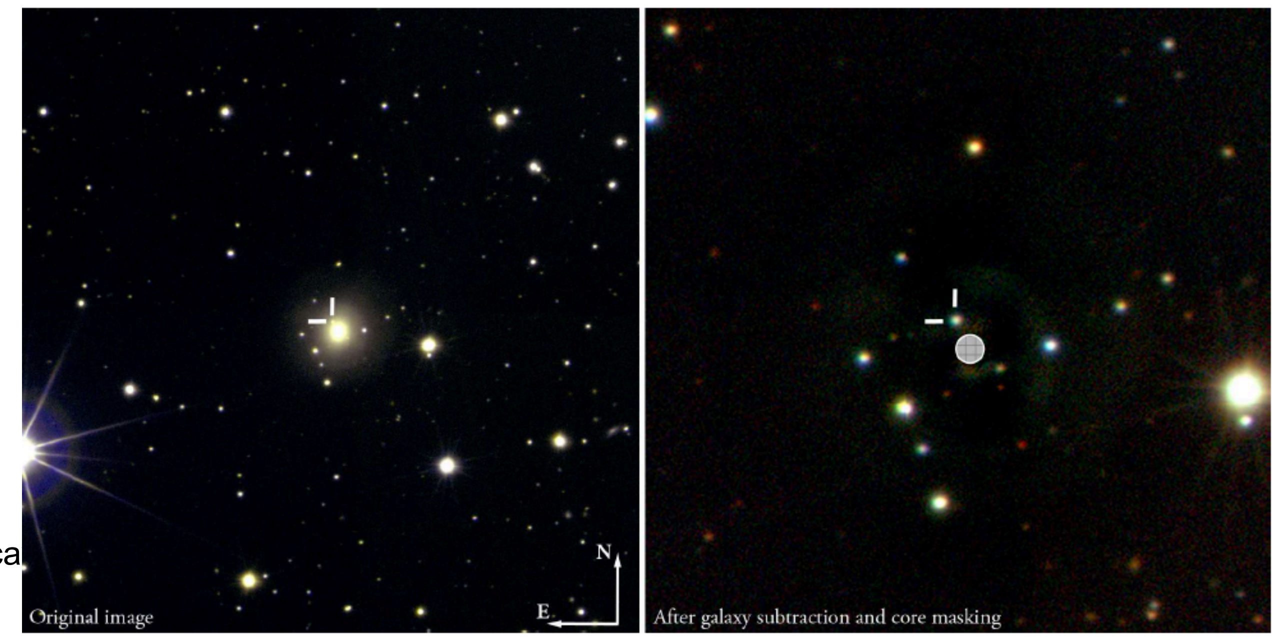

Figure 1. Left: pseudo-color image of a small subsection (9.′5 on a side) of the FoV of T80S, centered on the transient. Intensity scaling is logarithmic in order to better display the light distribution of the host galaxy. Right: 3× zoom into the residual image after host galaxy subtraction and core masking (hatched circle; see §2.2 for details).

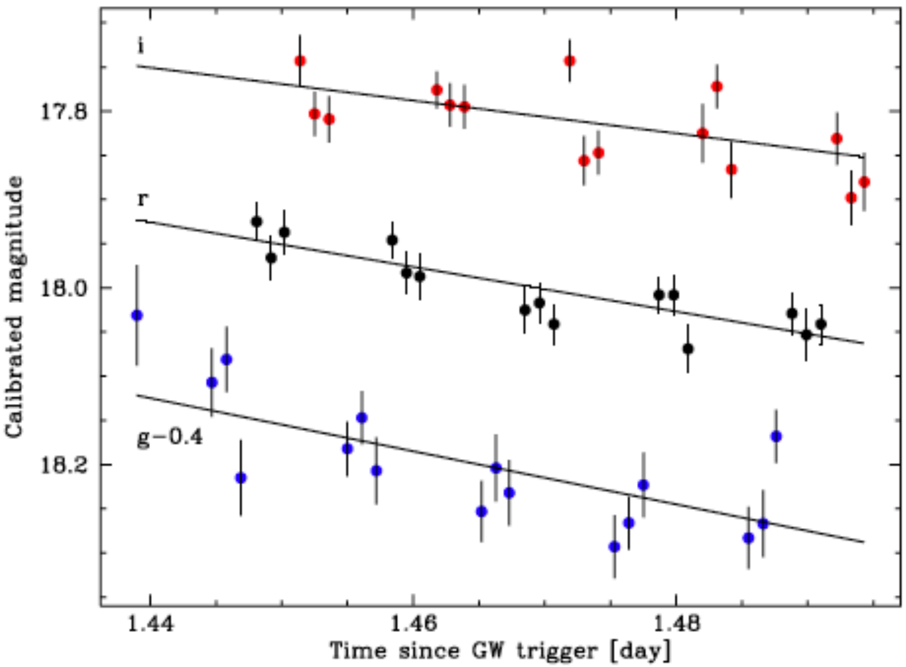

Figure 2. *gri* light curves of the EM counterpart to GW170817, obtained with T80S on 2017 August 18. The g points have been offset by -0.4 mag for clarity.

Table 1. Time-series photometry

Time[a]	Band	Mag	σ (mag)
1.4390	g	18.43 0.06	
1.4447	g	18.51 0.04	
1.4458	g	18.48 0.04	
1.4469	g	18.62 0.04	
1.4481	r	17.93 0.02	
1.4492	r	17.97 0.02	
1.4502	r	17.94 0.02	
1.4514	i	17.74 0.03	

NOTE—*a*: days since GW trigger.

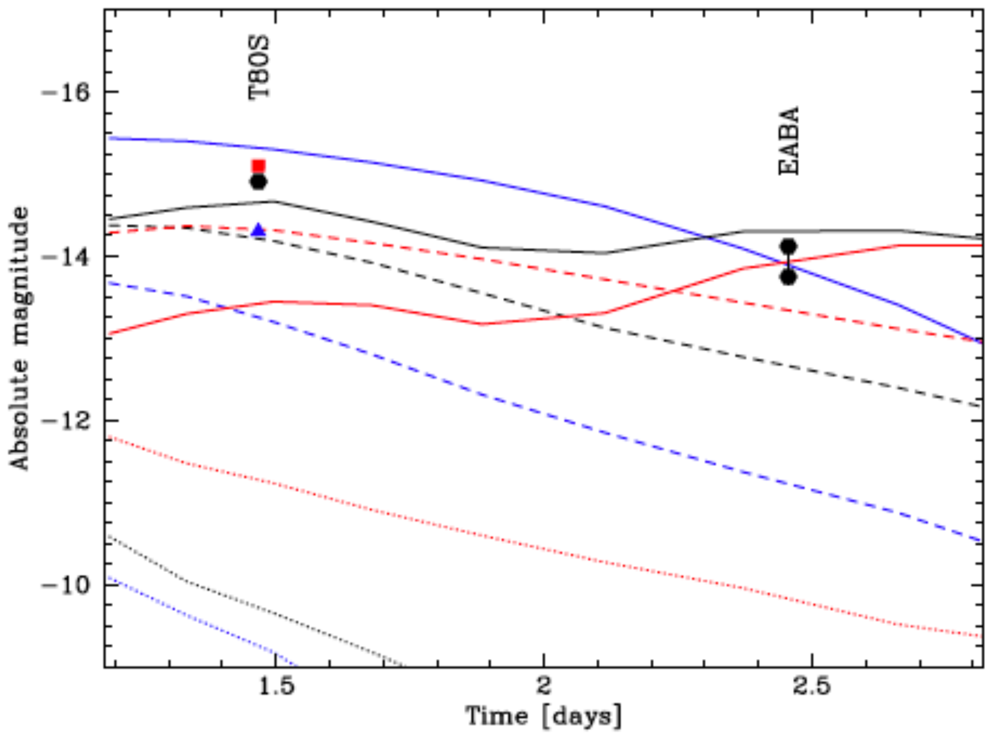

Figure 4. Comparison of our photometry (g: blue triangle; r: black hexagons; i: red square) adjusted to $D = 38$ Mpc with models from Tanaka et al. (2017) plotted using the same color scheme. The dotted lines represent a "red kilonova" model with dynamical ejecta rich in lanthanides. The dashed and solid lines represent "blue kilonova" wind models with decreasing amounts of lanthanides. The measurement uncertainties are smaller than the size of the symbols. The two possible r values at 2.456 days are discussed in §3.

LCO light curves of the kilonova AT 2017gfo

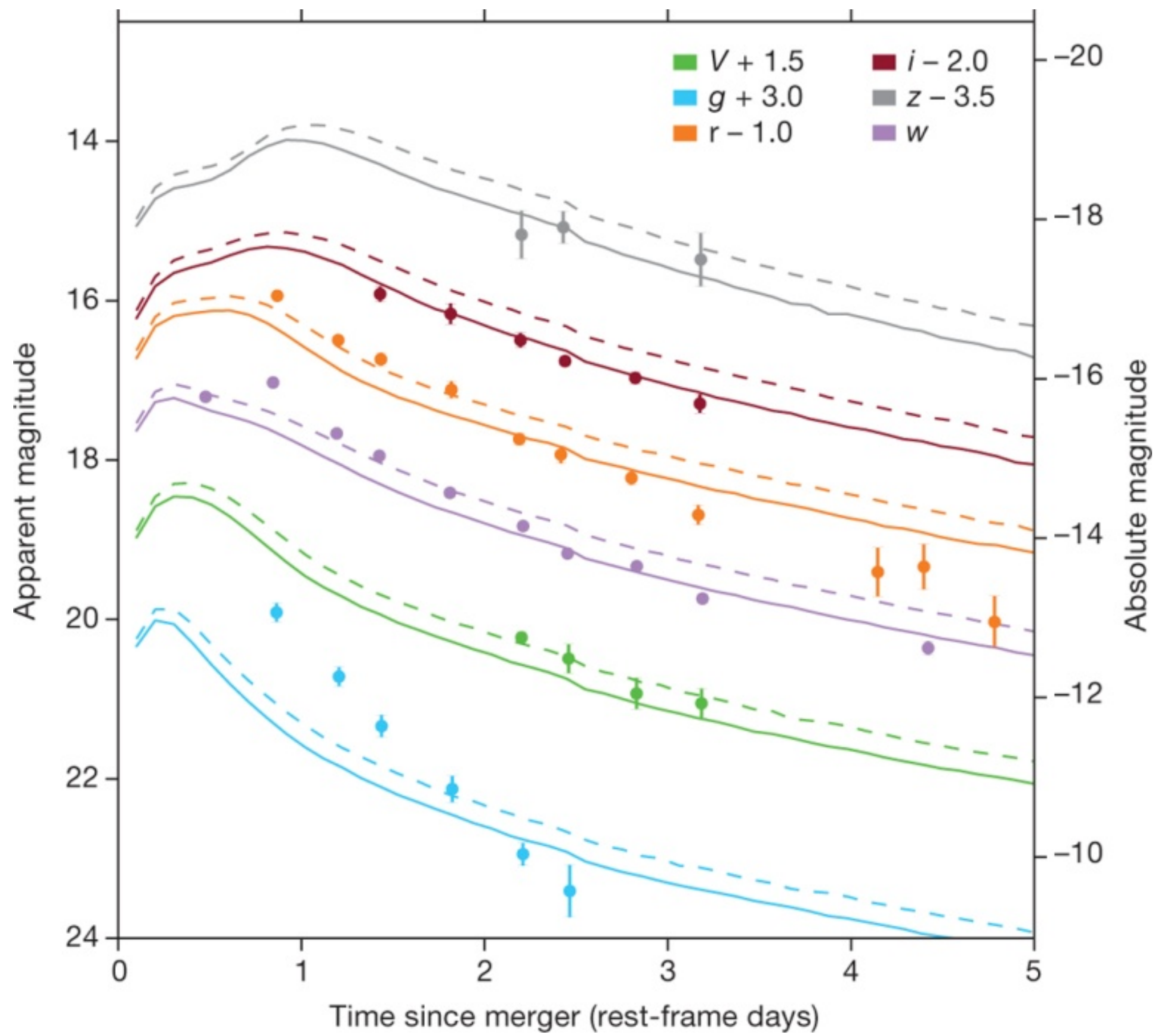

I Arcavi *et al.* *Nature* 1–3 (2017) doi:10.1038/nature24291

nature

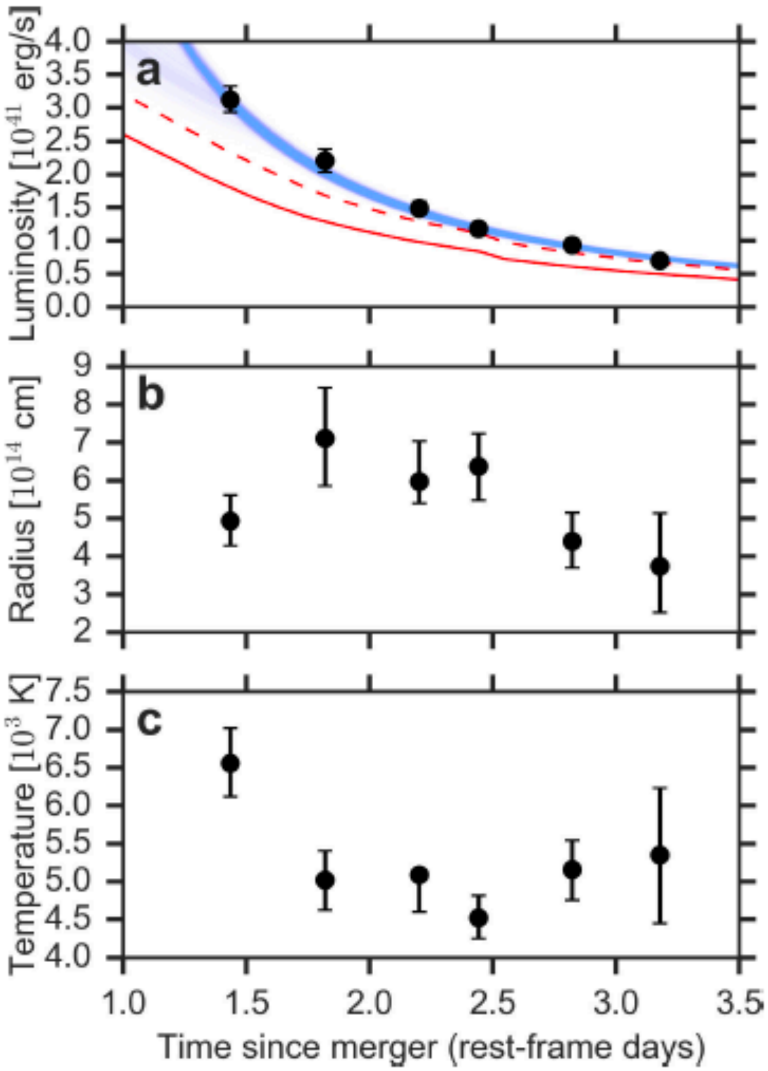

Extended Data Figure 3 | Bolometric luminosity, photospheric radius and temperature deduced from blackbody fits. Error bars denote 1σ uncertainties ($n = 200$). The large uncertainties in the later epochs might be due to a blackbody that peaks redward of our available data, so these data points should be considered to be temperature upper limits. Our MCMC fits of an analytical model[32] to the bolometric luminosity are shown in blue, and the numerical models[21] from Fig. 3 are shown in red in the top panel. The numerical models were tailored to fit *Vriw* bands, but not the *g* band, which is driving the high bolometric luminosity at early times.

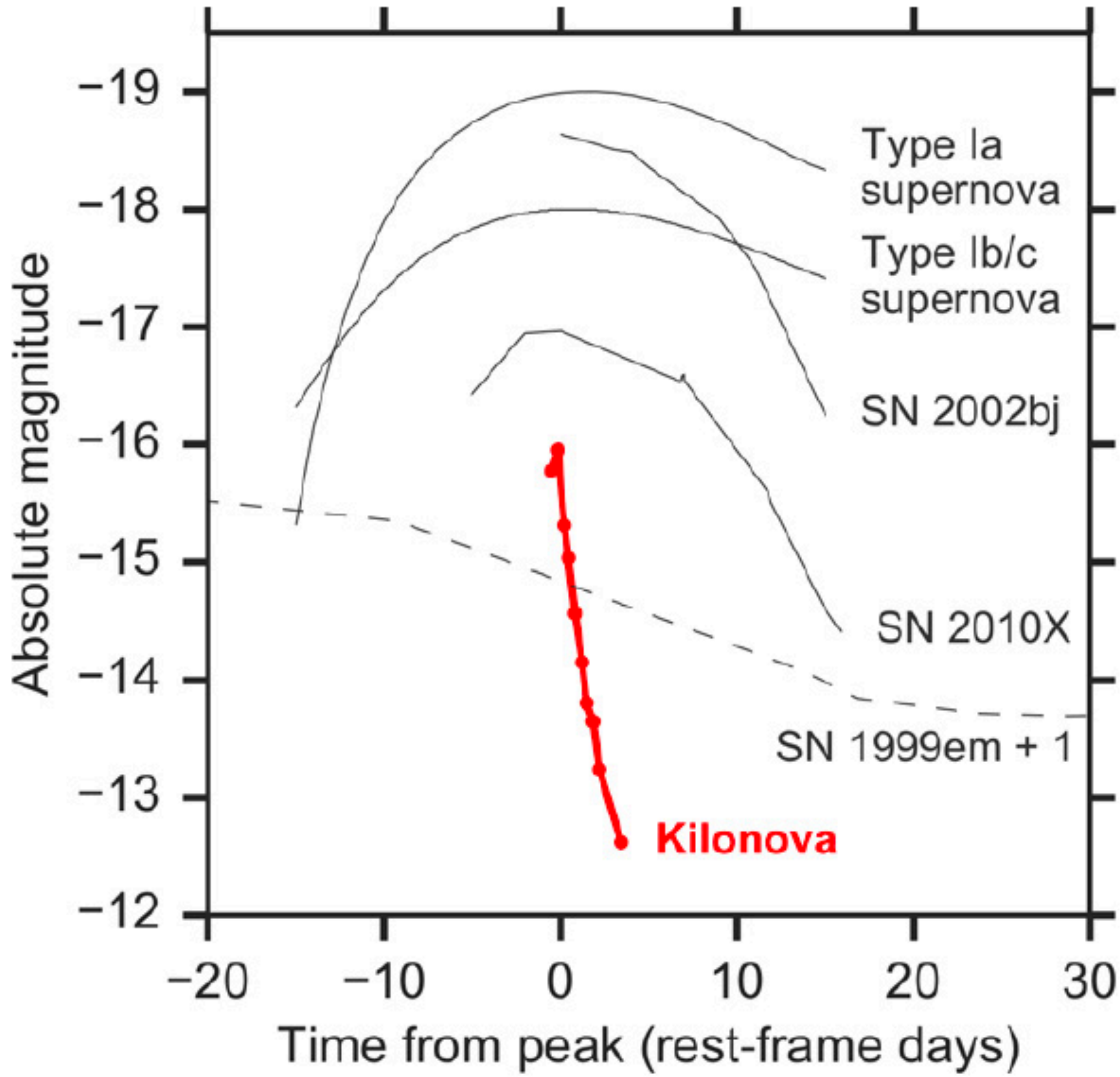

Extended Data Figure 4 | AT 2017gfo evolves faster than any known supernova, contributing to its classification as a kilonova. We compare our *w*-band data of AT 2017gfo (red; arrows denote 5σ non-detection upper limits reported by others[55,56]) to *r*-band templates of common supernova types (types Ia and Ib/c normalized to peaks of −19 mag and −18 mag, respectively)[50,51], to *r*-band data of two rapidly evolving supernovae[52,53] (SN 2002bj and SN 2010X) and to *R*-band data of the drop from the plateau of the prototypical type IIP supernova[54] SN 1999em (dashed line; shifted by 1 mag for clarity).

LETTER

doi:10.1038/nature24298

Spectroscopic identification of r-process nucleosynthesis in a double neutron-star merger

E. Pian[1], P. D'Avanzo[2], S. Benetti[3], M. Branchesi[4,5], E. Brocato[6], S. Campana[2], E. Cappellaro[3], S. Covino[2], V. D'Elia[6,7], J. P. U. Fynbo[8], F. Getman[9], G. Ghirlanda[2], G. Ghisellini[2], A. Grado[9], G. Greco[10,11], J. Hjorth[8], C. Kouveliotou[12], A. Levan[13], L. Limatola[9], D. Malesani[8], P. A. Mazzali[14,15], A. Melandri[2], P. Møller[16], L. Nicastro[1], E. Palazzi[1], S. Piranomonte[6], A. Rossi[1], O. S. Salafia[2,17], J. Selsing[8], G. Stratta[10,11], M. Tanaka[18], N. R. Tanvir[19], L. Tomasella[3], D. Watson[8], S. Yang[20,21], L. Amati[1], L. A. Antonelli[6], S. Ascenzi[6,22,23], M. G. Bernardini[2,24], M. Boër[25], F. Bufano[26], A. Bulgarelli[1], M. Capaccioli[9,27], P. Casella[6], A. J. Castro-Tirado[28], E. Chassande-Mottin[29], R. Ciolfi[3,30], C. M. Copperwheat[14], M. Dadina[1], G. De Cesare[1], A. Di Paola[6], Y. Z. Fan[31], B. Gendre[32], G. Giuffrida[6], A. Giunta[6], L. K. Hunt[33], G. L. Israel[6], Z.-P. Jin[31], M. M. Kasliwal[34], S. Klose[35], M. Lisi[6], F. Longo[36], E. Maiorano[1], M. Mapelli[3,37], N. Masetti[1,38], L. Nava[2,39], B. Patricelli[40], D. Perley[14], A. Pescalli[2,41], T. Piran[42], A. Possenti[43], L. Pulone[6], M. Razzano[40], R. Salvaterra[44], P. Schipani[9], M. Spera[3], A. Stamerra[40,45], L. Stella[6], G. Tagliaferri[2], V. Testa[6], E. Troja[46], M. Turatto[3], S. D. Vergani[2,47] & D. Vergani[1]

The merger of two neutron stars is predicted to give rise to three major detectable phenomena: a short burst of γ-rays, a gravitational-wave signal, and a transient optical–near-infrared source powered by the synthesis of large amounts of very heavy elements via rapid neutron capture (the r-process)[1–3]. Such transients, named 'macronovae' or 'kilonovae'[4–7], are believed to be centres of production of rare elements such as gold and platinum[8]. The most compelling evidence so far for a kilonova was a very faint near-infrared rebrightening in the afterglow of a short γ-ray burst[9,10] at redshift $z = 0.356$, although findings indicating bluer events have been reported[11]. Here we report the spectral identification and describe the physical properties of a bright kilonova associated with the gravitational-wave source[12] GW170817 and γ-ray burst[13,14] GRB 170817A associated with a galaxy at a distance of 40 megaparsecs from Earth. Using a series of spectra from ground-based observatories covering the wavelength range from the ultraviolet to the near-infrared, we find that the kilonova is characterized by rapidly expanding ejecta with spectral features similar to those predicted by current models[15,16]. The ejecta is optically thick early on, with a velocity of about 0.2 times light speed, and reaches a radius of about 50 astronomical units in only 1.5 days. As the ejecta expands, broad absorption-like lines appear on the spectral continuum, indicating atomic species produced by nucleosynthesis that occurs in the post-merger fast-moving dynamical ejecta and in two slower (0.05 times light speed) wind regions. Comparison with spectral models suggests that the merger ejected 0.03 to 0.05 solar masses of material, including high-opacity lanthanides.

GW170817 was detected on 17 August 2017, 12:41:04 universal time (UT)[12]. A weak, short-duration ($t \approx 2$ s) γ-ray burst (GRB) in the gravitational-wave error region triggered the Fermi GRB monitor (Fermi-GBM) about two seconds later[13], and was detected also by INTEGRAL SPI-ACS (spectrometer on the International Gamma-Ray Astrophysics Laboratory (INTEGRAL) anticoincidence system)[14] (see also Zhang, B.-B. *et al.*, manuscript in preparation). Considerably improved sky localization was obtained from the joint analysis of LIGO and Virgo data of the gravitational-wave event, with a 90% error region of 33.6 square degrees (ref. 12). This joint gravitational-wave/GRB detection was followed by an extensive worldwide observational campaign using space- and ground-based telescopes to scan the sky region were the events were detected. A new point-like optical source (coordinates right ascension α(J2000) = 13 h 09 min 48.09 s, declination δ(J2000) = −23° 22′ 53.3″) was soon reported[17,18], located at 10 arcsec from the centre of the S0 galaxy NGC 4993 ($z = 0.00968$; ref. 19) in the ESO 508-G018 group and at a distance of 40 Mpc from Earth, consistent with the luminosity distance of the gravitational-wave signal. It was

[1]INAF, Institute of Space Astrophysics and Cosmic Physics, Via Gobetti 101, I-40129 Bologna, Italy. [2]INAF, Osservatorio Astronomico di Brera, Via E. Bianchi 46, I-23807 Merate, Italy. [3]INAF, Osservatorio Astronomico di Padova, Vicolo dell'Osservatorio 5, I-35122 Padova, Italy. [4]Gran Sasso Science Institute, Viale F. Crispi 7, L'Aquila, Italy. [5]INFN, Laboratori Nazionali del Gran Sasso, I-67100 L'Aquila, Italy. [6]INAF, Osservatorio Astronomico di Roma, Via di Frascati 33, I-00078 Monteporzio Catone, Italy. [7]Space Science Data Center, ASI, Via del Politecnico, 00133 Roma, Italy. [8]Dark Cosmology Centre, Niels Bohr Institute, University of Copenhagen, Juliane Maries Vej 30, DK-2100 Copenhagen Ø, Denmark. [9]INAF, Osservatorio Astronomico di Capodimonte, salita Moiariello 16, I-80131 Napoli, Italy. [10]Università degli Studi di Urbino 'Carlo Bo', Dipartimento di Scienze Pure e Applicate, Piazza Repubblica 13, I-61029 Urbino, Italy. [11]INFN, Sezione di Firenze, I-50019 Sesto Fiorentino, Italy. [12]Astronomy, Physics, and Statistics Institute of Sciences (APSIS) and Department of Physics, The George Washington University, Corcoran Hall, Washington DC 20052, USA. [13]Department of Physics, University of Warwick, Gibbet Hill Road, Coventry CV4 7AL, UK. [14]Astrophysics Research Institute, Liverpool John Moores University, Liverpool Science Park, IC2, 146 Brownlow Hill, Liverpool L3 5RF, UK. [15]Max-Planck-Institut für Astrophysik, Karl-Schwarzschild-Strasse 1, 85748 Garching bei München, Germany. [16]European Southern Observatory, Karl-Schwarzschild-Strasse 2, D-85748 Garching bei München, Germany. [17]Dipartimento di Fisica 'G. Occhialini', Università degli Studi di Milano-Bicocca, Piazza della Scienza 3, I-20126 Milano, Italy. [18]National Astronomical Observatory of Japan, Mitaka, Tokyo, Japan. [19]Department of Physics and Astronomy, University of Leicester, University Road, Leicester LE1 7RH, UK. [20]Department of Astronomy and Physics, Padova University, Padova, Italy. [21]Department of Astronomy, University of California, Davis, California, USA. [22]Dipartimento di Fisica, Università di Roma La Sapienza, Piazzale Aldo Moro 2, I-00185 Roma, Italy. [23]Università di Roma Tor Vergata, Via della Ricerca Scientifica 1, I-00133 Roma, Italy. [24]Laboratoire Univers et Particules de Montpellier, Université Montpellier, CNRS/IN2P3, Montpellier, France. [25]ARTEMIS (UCA, CNRS, OCA), Boulevard de l'Observatoire, CS 34229, F-06304 Nice Cedex 4, France. [26]INAF — Osservatorio Astronomico di Catania, Via S. Sofia 78, I-95123 Catania, Italy. [27]Department of Physics, University of Naples Federico II, Corso Umberto I 40, 80138 Napoli, Italy. [28]Instituto de Astrofísica de Andalucía (CSIC), Glorieta de la Astronomía, E-18008 Granada, Spain. [29]APC, Université Paris Diderot, CNRS/IN2P3, CEA/Irfu, Observatoire de Paris, Sorbonne Paris Cité, France. [30]INFN-TIFPA, Trento Institute for Fundamental Physics and Applications, Via Sommarive 14, I-38123 Trento, Italy. [31]Key Laboratory of Dark Matter and Space Astronomy, Purple Mountain Observatory, Chinese Academy of Science, Nanjing 210008, China. [32]University of Virgin Islands, 2 John Brewer's Bay, St Thomas, Virgin Islands 00802, USA. [33]INAF — Osservatorio Astrofisico di Arcetri, Largo Enrico Fermi 5, I-50125 Florence, Italy. [34]Division of Physics, Mathematics and Astronomy, California Institute of Technology, Pasadena, California 91125, USA. [35]Thüringer Landessternwarte Tautenburg, Sternwarte 5, D-07778 Tautenburg, Germany. [36]University of Trieste and INFN Trieste, I-34127 Trieste, Italy. [37]Institute for Astrophysics and Particle Physics, University of Innsbruck, Technikerstrasse 25/8, A-6020 Innsbruck, Austria. [38]Departamento de Ciencias Físicas, Universidad Andrés Bello, Fernández Concha 700, Las Condes, Santiago, Chile. [39]INAF, Osservatorio Astronomico di Trieste, Via G.B. Tiepolo 11, I-34143 Trieste, Italy. [40]Scuola Normale Superiore, Piazza dei Cavalieri 7, I-56126 Pisa, Italy. [41]Università degli Studi dell'Insubria, via Valleggio 11, I-22100 Como, Italy. [42]Racah Institute of Physics, The Hebrew University of Jerusalem, Jerusalem 91904, Israel. [43]INAF, Osservatorio Astronomico di Cagliari, Via della Scienza 5, I-09047 Selargius, Italy. [44]INAF, Istituto di Astrofisica Spaziale e Fisica Cosmica di Milano, via E. Bassini 15, I-20133 Milano, Italy. [45]INAF, Osservatorio Astronomico di Torino, Pino Torinese, Italy. [46]NASA, Goddard Space Flight Center, Greenbelt, Maryland 20771, USA. [47]GEPI, Observatoire de Paris, PSL Research University, CNRS, Place Jules Janssen, 92190 Meudon, France.

So far the most interesting result

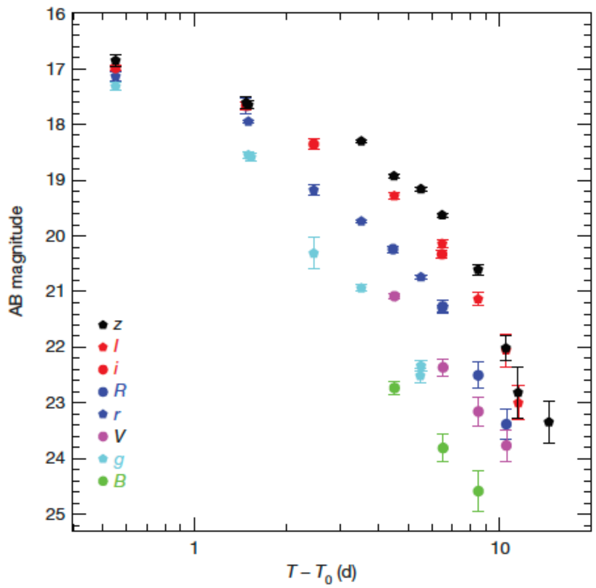

Figure 1 | Multiband optical light curve of AT 2017gfo. The data shown for each filter (see legend) are listed in Extended Data Table 1. Details of data acquisition and analysis are reported in Methods. The *x* axis indicates the difference in days between the time at which the observation was carried out *T* and the time of the gravitation-wave event T_0. The error bars show the 1σ confidence level. The data have not been corrected for Galactic reddening.

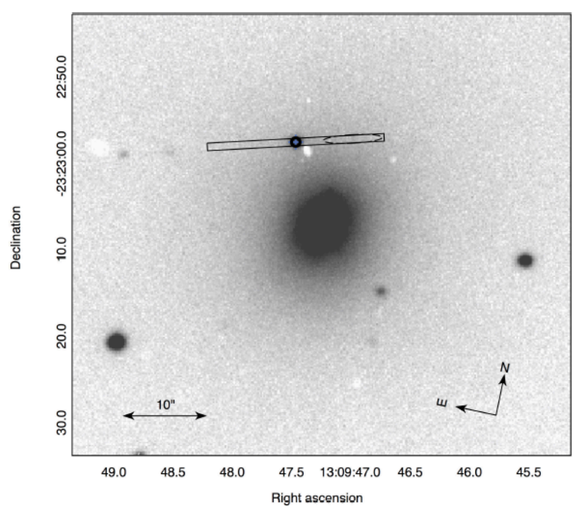

Extended Data Figure 1 | Image of the NGC 4993 galaxy . The image was obtained with the X-shooter acquisition camera (*z* filter). The X-shooter slit is overlaid as a rectangle. The position of the optical transient is marked by a blue circle. The position of the line emission in the slit is marked by an ellipse. The dust lanes that are visible in the host intersect the slit at the position of the line emission.

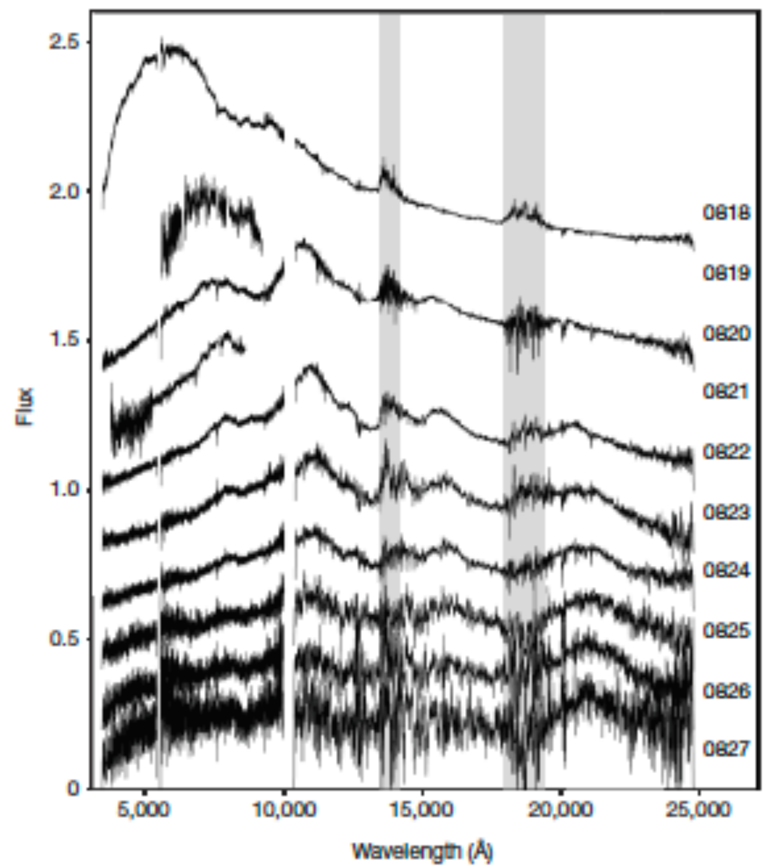

Figure 2 | Time evolution of the AT 2017gfo spectra. VLT/X-shooter, VLT/FORS2 and Gemini/GMOS spectra of AT 2017gfo. Details of data acquisition and analysis are reported in Methods. For each spectrum, the observation epoch is reported on the left (phases with respect to the gravitation-wave trigger time are reported in Extended Data Table 2; the flux normalization is arbitrary). Spikes and spurious features were removed and a filter median of 21 pixels was applied. The shaded areas mark the wavelength ranges with very low atmospheric transmission. The data have not been corrected for Galactic reddening.

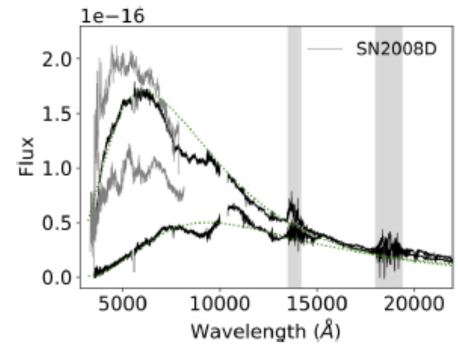

Extended Data Figure 2 | Blackbody fit to the AT 2017gfo spectra. The two early X-shooter spectra of GW170817, obtained 1.5 and 3.5 days after discovery, are compared with the spectra of the type-Ib supernova SN 2008D[59], obtained 2–5 days after the explosion (light grey, arbitrarily scaled in flux, $\times 10^{-16}$). The shaded areas represent wavelength intervals with low atmospheric transmission. The dotted green lines show the black-body fits of the optical continuum of GW170817 with temperature 5,000 K and 3,200 K.

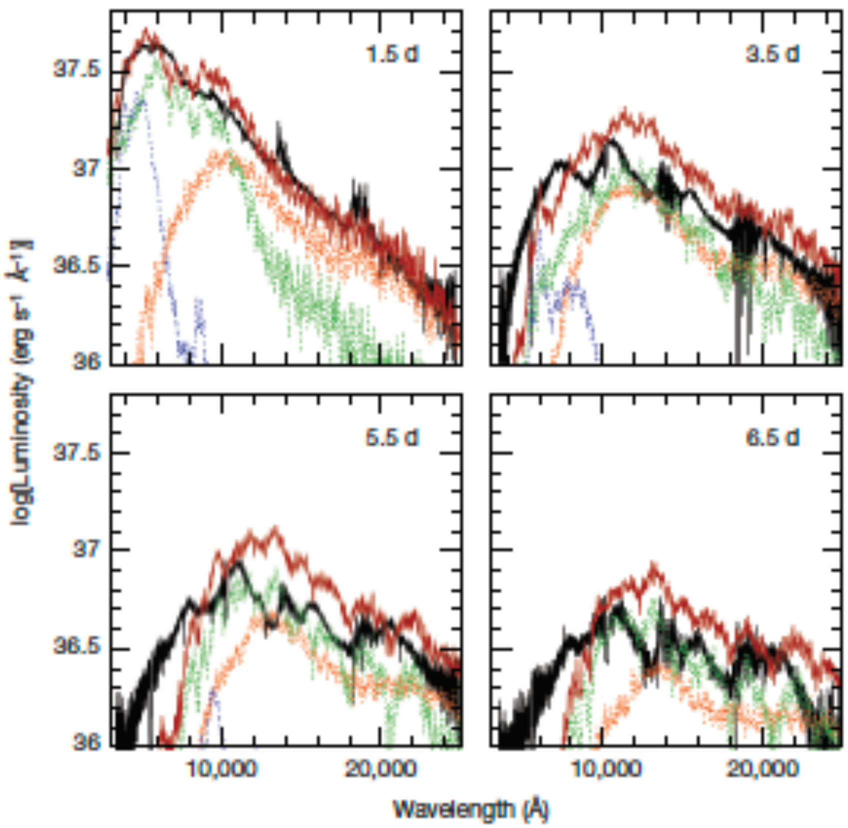

Figure 3 | Kilonova models compared with the AT 2017gfo spectra. X-shooter spectra (black line) at the first four epochs and kilonova models: dynamical ejecta ($Y_e = 0.1$–0.4, orange), wind region with proton fraction $Y_e = 0.3$ (blue) and $Y_e = 0.25$ (green). The red curve represents the sum of the three model components.

- The two main n-capture processes were first identified by Burbidge et al. 1957.

- They are the slow (s) and rapid (r) processes:
  the s- and r-processes.

- In the s-process the neutron capture happens in a time scale (τ_n) much longer than the mean time for β-decay (τ_β), i.e., $\tau_n >> \tau_\beta$.
- In the case of the r-process: $\tau_n << \tau_\beta$.
- While τ_β depends only on the nuclear species, τ_n depends strongly on the environment, specifically on a strong neutron flux.

- The strong flux of neutron is a transient phenomena. After it stops, the nuclei will β decay until they reach the valley of stability. The magenta points show stable nuclei produced by the r-process.
- The black points mark the elements made by mainly the **s-processes**.
- The solar system elements are an admixture of s- and r-process elements (~50/50).
- Jeweler's elements like gold and platinum are made almost exclusively by the r-process.

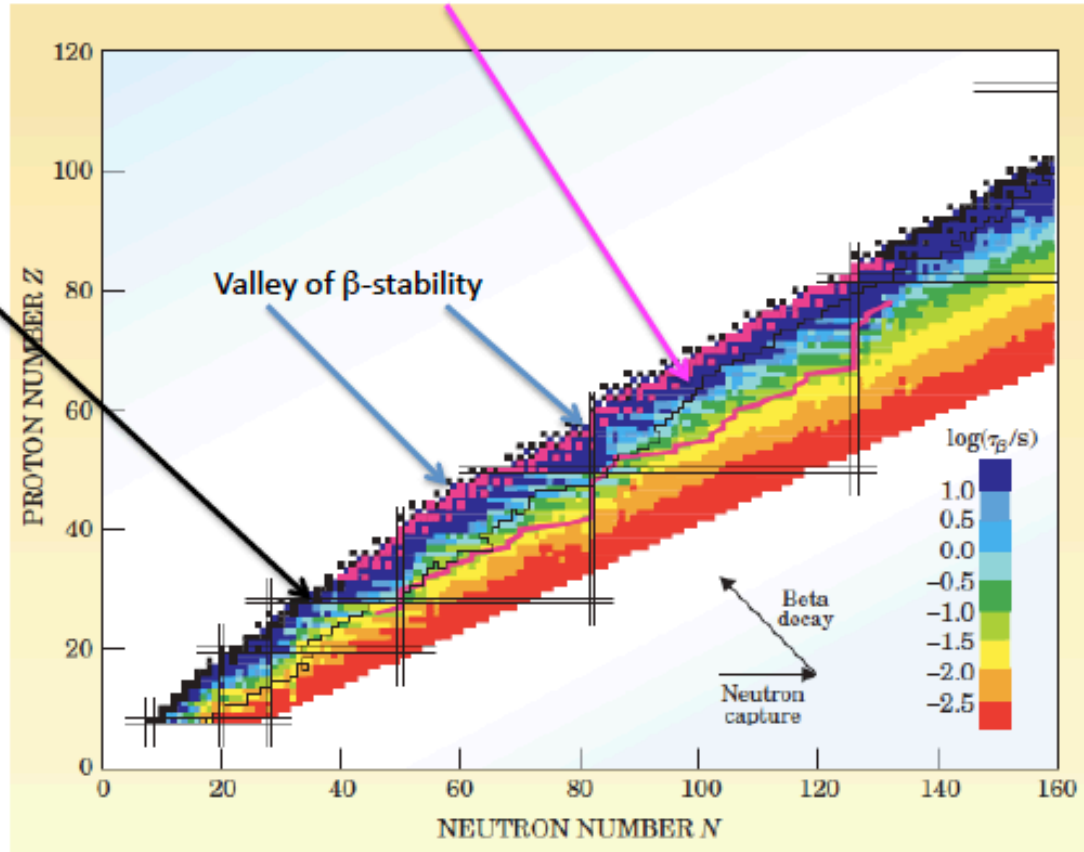

- The s-process is relatively well understood.
- The nuclear properties of the involved species that are easier to measure in the lab than the ones of the r-process (longer τ_β).
- The site is also much better constrained: primarily low- and intermediate-mass stars (less than 8 solar masses).
- The r-process element formation is much more uncertain.
- The nuclear properties of the participating elements is much more difficult to measure.
- And the sites where the r-process take place are a mistery. Not anymore
- R-process element formation requires large neutron fluxes that are associated to rather catastrophic events. The two main candidates are **type II (core-collapse) supernova explosions** and **neutron star mergers**. At present the astrophysical conditions of these two phenomena are not well understood (good review: Sneden et al. 2003).

An International Network of Interferometers

Simultaneously detect signal (within msec)

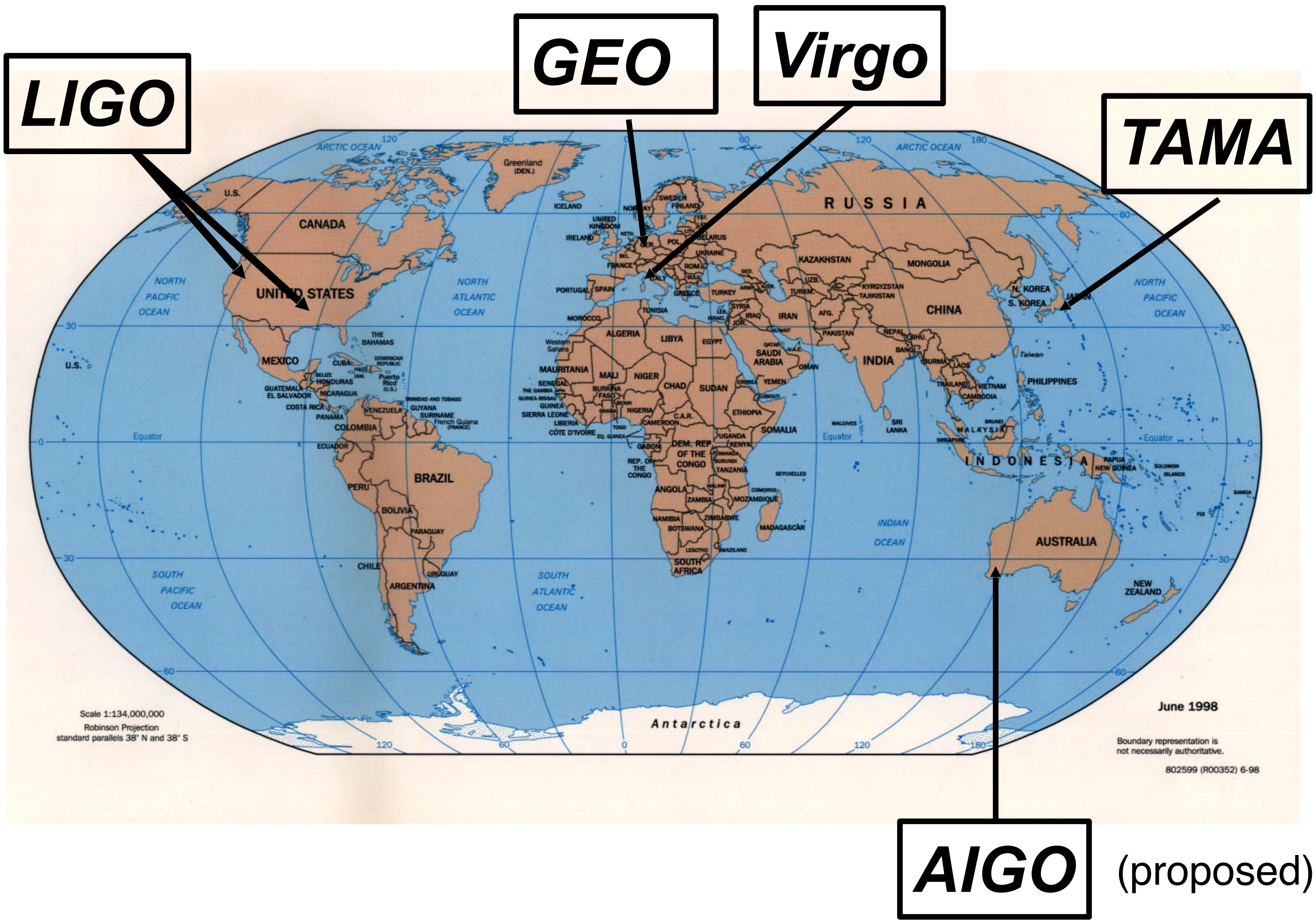

detection confidence

locate the sources

decompose the polarization of gravitational waves

We got the infrastructure

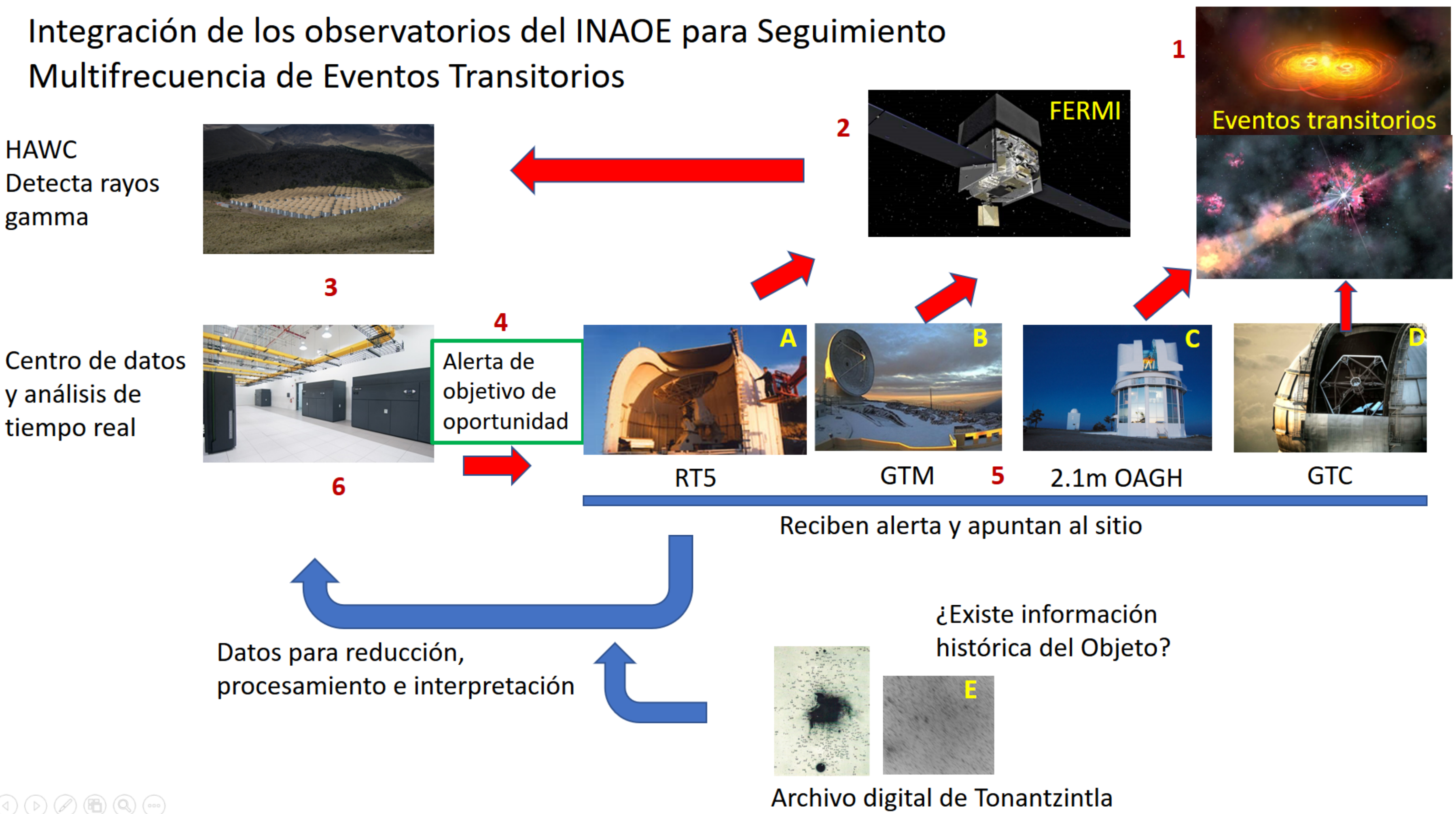

Red Tematica Conacyt: Agujeros negros y ondas Gravitatorias

Several groups in NR

ICN-UNAM
Miguel Alcubierre (binaries)
Dario Nunez
(Post Mergers, multimessenger)
Marcelo Salgado (Neutron stars)

Cinvestav
Tonatiuh Matos
(Compact objects mimickers)

UMSH
Francisco Siddhartha
(binaries, accretion)
Jose Antonio Gonzalez
(binaries, accretion)
Oliver Sarbach
(Post mergers, Foundations)

UdG
Claudia Moreno
(Perturbation theory)

ICF-UNAM,
JCD
(Post mergers, multimessenger, BH instabilities)

INAOE
Omar Lopez
(Observation, EHT)

This is a new era for the exploration of the universe